TOWARDS 21% EFFICIENT N-CZ IBC BASED ON SCREEN PRINTING

M.W.P.E. Lamers[1], A.A. Mewe[1], I.G. Romijn[1], E.E. Bende[1], Y. Komatsu[1], M. Koppes[1],
D. Morecroft[2], M. Cascant[2], F.J. Castaño[2], A.W. Weeber[1], I. Cesar[1]
[1]ECN Solar Energy, P.O. Box 1, NL-1755 ZG Petten, the Netherlands
[2]Siliken Renewable Energy, Department of R&D, Ciudad Politécnica de la Innovación – UPV,
Camino de Vera, 14 (46022) Valencia, Spain.
Tel: +31 224 564217, Fax: +31 224 56 8214, Email: Cesar@ecn.nl

ABSTRACT: Interdigitated Back Contact (IBC) cells have been fabricated at ECN laboratories with a best cell efficiency of 19.1%, using n-type Cz material and a process flow based on all-screen-printed patterning and metallization. Excellent current collection due to an optimized FSF is demonstrated by a J_{sc} value as high as 41.5 mA/cm^2, corrected for spectral mismatch, and a V_{oc} of 641 mV. The results show high Pseudo Fill Factors (*PFF*) of above 81% but lower Fill Factors (*FF*) of below 72%.
Keywords: back contact, silicon solar cell, high-efficiency

1 INTRODUCTION

Driven by market pressure to increase cell efficiencies and decrease production costs, we have developed a process flow for Interdigitated Back Contact (IBC) cells that is compatible with low-cost industrial processes. The process flow comprises conventional screen-printing steps for patterning and metallization, avoiding more expensive approaches such as lithography [1-3].

High efficiencies (>20%) can be achieved in IBC cells mainly because all current collection contacts are located at the rear, which eliminates the problem of front shading losses. A schematic cross section of the IBC cell can be seen in figure 1. Although optical shading losses are eliminated, recombination losses occur in the regions without emitter as the transport towards the emitter becomes comparable to the local diffusion length. This effect is referred to as electrical shading [4]. To reach the high cell efficiencies, the device structure requires excellent surface passivation at the front and rear sides, as well as patterning of both n- and p-type regions at the rear of the cell and a high bulk lifetime (>1 ms). Narrow and abrupt contact areas will result in reduced resistive and lateral losses. These losses are determined by the minimum feature size, which is limited by the patterning method used. The top-down solution of lithography is able to achieve close to ideal contact regions but the current process is too expensive for high-volume manufacturing. On the bottom-up end, screen-printing is well demonstrated in PV manufacturing and it is therefore important to evaluate the limits in the efficiencies of IBC cells fabricated using this approach.

Since the emitter in IBC cells is located at the rear, an almost ideal surface passivation is required at the front as most charge carriers are created close to that interface. The formation of a high-quality Front Surface Field (FSF) is necessary, which should provide a shielding field effect with no added Auger recombination and can be passivated using a dielectric layer.

In this paper we present the IBC cell made at ECN using tube furnace diffusions, wet-chemical, PECVD and screen-printing (patterning and metallization) process steps alone. The efficiency limits of the fabrication process presented are evaluated by studying the influence of the pitch and emitter fraction, and the effect of unpassivated contacts.

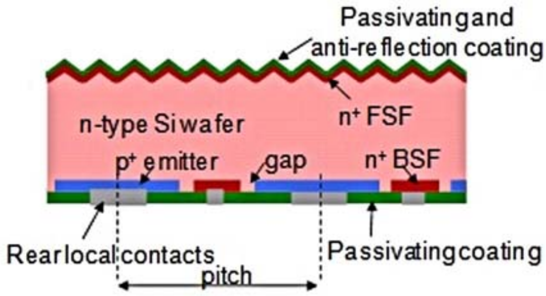

Figure 1: Schematic of an IBC cell, indicating the Front Surface Field (FSF), n$^+$-Back Surface Field (BSF), p$^+$ -emitter, contacts and passivating layers. The definition of pitch and gap are also included. All contacts are located at the rear.

2 SOLAR CELL AND PROCESS DESCRIPTION

In figure 2 the process flow used to fabricate the IBC cells at ECN is shown. To enable optimal light confinement, the front surface of the cells is textured (random pyramids) using alkaline etching while the rear surface is smoothened which also improves passivation. This wet-chemical process is followed by the FSF diffusion, mainly to reduce the recombination at the front side [5]. After FSF diffusion, the steps include masking, diffusion and patterning of the boron emitter and phosphorus BSF at the rear surface. The emitter and BSF are separated by a non-diffused gap, to avoid shunting. To ensure high efficiencies, front and rear side passivation needs to be excellent. The IBC cells require a rear surface passivation solution for three different surfaces: the highly doped p-type emitter, the highly doped n-type back surface field and the lightly doped n-type base. For this, the full rear side is passivated using a stack of SiO_2/SiN_x:H. The front side is passivated using SiN_x:H coating on top of the FSF. Subsequently, metallization on the BSF and emitter regions is done by screen printing and contacting of both regions is achieved simultaneously by a short high temperature firing step. All patterning and metallization steps were executed using low-cost screen-printing methods. Contacting was achieved by so-called firing-through using an inline belt furnace. The metallization fraction on the rear side was varied between 7.5 and 11.3%, excluding busbars, depending on the pitch.

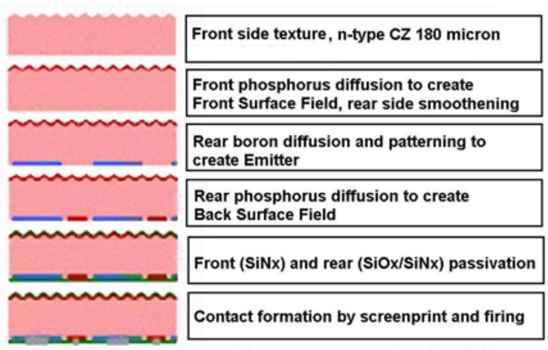

Figure 2: Process flow used for fabricating >19% interdigitated back contact solar cells at ECN.

3 SOLAR CELL OPTIMIZATION

Several aspects of the IBC solar cell can be optimized and in this paper results of various optimizations are presented. These include the FSF, the pitch and the emitter fraction. For the fabrication of the cells 3-4 Ωcm n-type Cz grown Si material was used, for which the bulk lifetime exceeded 1 ms.

3.1 Front surface field optimization

The function of the front surface is to reduce the recombination at the front side and improve lateral transport. Recombination in the FSF should be minimal and the optimal doping level was found to be 3.10^{18} atoms/cm^2 [6-8]. Improved lateral tranport by the FSF becomes increasingly important for larger pitches and higher base resistivity. For this, the optimal resistance was found to be 150 Ω/sq for the FSF. These specifications indicate that the FSF profile should be deep, close to 1µm. In order to fabricate this by diffusion in an industrial process, a long process time is required which is undesired. For moderate to low bulk resistances and small pitches the additional value of the FSF for lateral transport is of less importance. Under these circumstances, a lightly doped and shallow FSF, with a high resistance in combination with good surface passivation, will give the highest cell output [5]. These specifications allow a short diffusion time in an industrial process. At ECN simulations of the FSF and the related output of the IBC cell were modelled as a function of the surface doping level, depth and the surface recombination velocity at the Si-SiNx interface (*S*). For the simulations a pitch of 2 mm, emitter fraction of 90%, a bulk lifetime of 1 ms and a Gaussian diffusion profile of the FSF were assumed. In figure 3 and 4 these modelling results are given for the FSF with a depth of 310 and 940 nm. It can be seen that the J_{sc} is optimal for dopants at 3.10^{18} atoms/cm^3 for a wide variety of *S* as it shows that for this doping level the processing is most stable in terms of surface passivation. It was found that J_{sc} decreases for doping levels below 1.10^{17} atoms/cm^3. The modelling also showed that for this surface doping level variations in depth of the FSF have not a significant effect on the J_{sc}. The modelling also shows that for a deeper FSF, J_{sc} more steeply declines for higher doping levels. This indicates that in processing a more superficial FSF is more stable and will lead to higher J_{sc} on average.

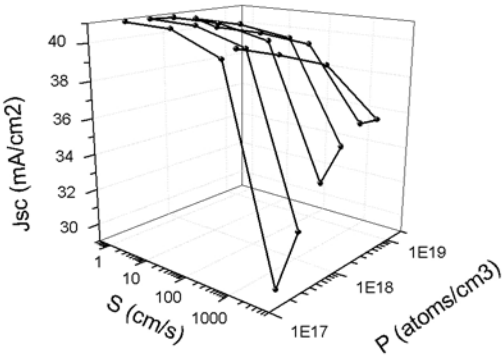

Figure 3: The relationship between the surface doping of the FSF (*P*), the surface recombination verlocity (*S*) and the J_{sc} for a FSF which is 310 nm deep.

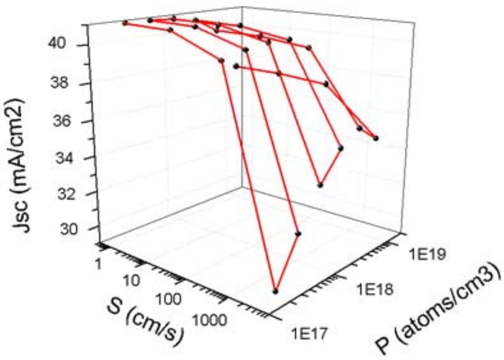

Figure 4: The relationship between the surface doping of the FSF (*P*), the surface recombination verlocity (*S*) and the J_{sc} for a FSF which is 940 nm deep.

Taking note of the increasing required processing time with increasing depth of the FSF and the more optimal process stability for a shallow FSF, it was therefore decided to use a shallow and a high resistance FSF with a surface doping level of 3.10^{18} atoms/cm^3 which had a J_{0e} of 44fA/cm^2 as measured on textured n-type Cz wafers. The sheet resistance was so high that it did not contribute to lateral transport.This FSF should lead to maximal J_{sc} and an optimal IQE.

3.2 Emitter fraction and pitch optimization

As shown in figure 1, the rear side consists of the BSF, the emitter and the gap. The fraction of each region can be varied. The fractions times the pitch give the widths of the different regions. We present here the average of 10 cells per pitch and per emitter fraction. In figures 5 and 6 the effect on the V_{oc} and J_{sc} for two different emitter fractions is given. A clear improvement in J_{sc} is found for a larger emitter fraction. This is due to a reduction in the recombination of the minority carriers as the collection area is increased and the required diffusion distance of the minority carriers is thus reduced. The values for V_{oc} are comparable to values found for other high efficiency screenprinted n-type Cz solar cells [9].

Using light beam induced current (LBIC) measurements, the Internal Quantum Efficiency (IQE) response of the cell at the back of the solar cell can be mapped. In figure 7 the IQE scan of one of the best IBC cells is shown for a wavelength of 976 nm. In figure 8 a line scan of this image is given. This cell had a pitch of

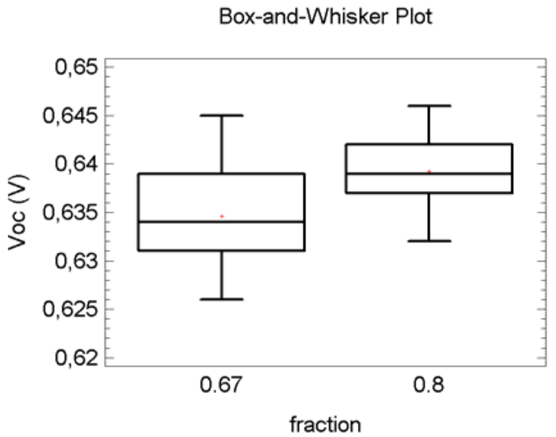

Figure 5: The effect on the V_{oc} for two different emitter fractions.

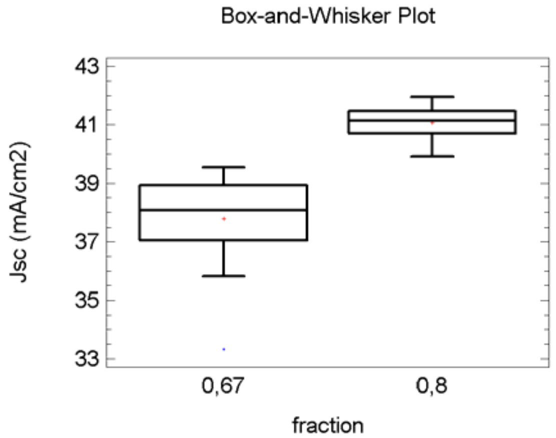

Figure 6: The effect on the J_{sc} for two different emitter fractions.

2 mm, an emitter fraction of 80% and a BSF and gap width of 400 µm. A high IQE of 97% can be seen in the region of the emitter (blue), in the region of the BSF this is 82% (orange/red), with intermediate values in the gap (green). This difference of 15% is due to the electrical shading losses. This is significant lower than was found by others who used a larger BSF and gap region [4,5]. The lower IQE in the BSF region indicates that the passivation needs to be improved. The high doping levels of the BSF, required for good contacting, reduce the passivation of this region [10].

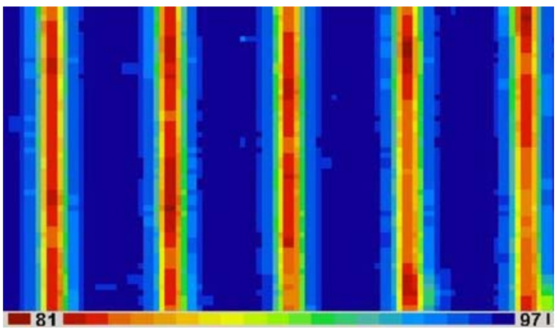

Figure 7. IQE measurement at 976 nm showing the local IQE. Highest IQE is shown in blue (emitter), lowest in red (BSF).

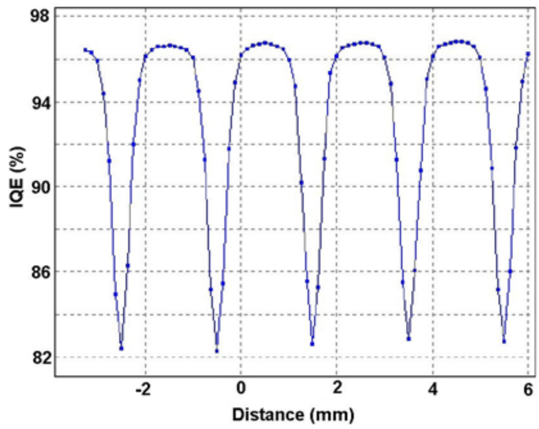

Figure 8. Line Scan of the IQE presented in figure 7. Highest IQE is found for the emitter, lowest for the BSF.

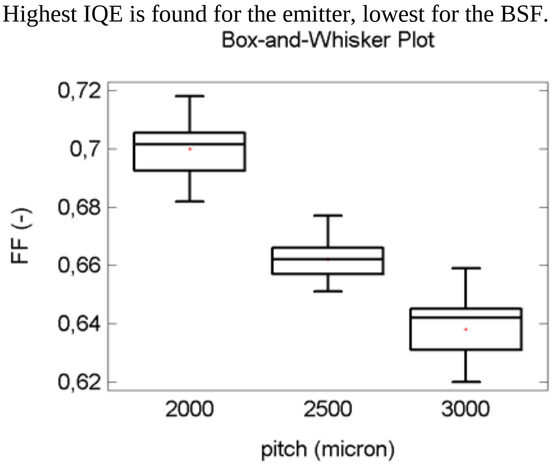

Figure 9: The effect on the *FF* for three different pitch.

In figure 9 the effect on the *FF* for three different pitches is given. No effect by the BSF width, gap width and emitter fraction on the *FF* was observed. A relatively low *FF* was found with a maximum value of 71.8%, which decreased as contact spacing increased. Combining commonly reported *FF* values of around 79% with he obtained values for J_{sc} and V_{oc} in this work, would result in cell efficiencies well above 21%. The low *FF* is currently subject of our research effort.

4 BEST CELL RESULTS

The overall experimental results show that several factors play an important role in obtaining high efficiency. These factors are high quality FSF, high emitter fraction and a small pitch. Figure 10 shows both (a) Internal Quantum Efficiency (IQE) and (b) IV data of our current best IBC cell. A summary of measured parameters corresponding to this best cell with 19.1% efficiency is given in Table 1. For this cell the emitter fraction was 80%, the pitch was 2 mm and the area 13.2 cm^2.

The IQE results are very good; approaching unity in a broad wavelength range, with characteristic drops in the blue response mainly due to absorption of light in the SiN_x layer, and in the red close to the band gap limit. Excellent current collection is shown by a J_{sc} value as high as 41.5 ± 1.2 mA/cm^2, as corrected for spectral mismatch. This J_{sc} is close to the maximal current which can be expected from IBC cells [5] and similar to what

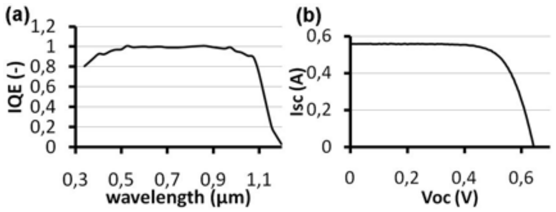

Figure 10: a) IQE, b) IV corresponding to the best IBC cell fabricated.

Table 1. Summary of the best cell parameters which gave an efficiency of 19.1%.

Pitch (mm)	Emitter fraction	J_{sc} (mA/cm^2)	V_{oc} (V)	*FF* (-)	*Eta* (%)
2	0.8	41.5	0.641	0.72	19.1

we obtain on Cz n-MWT cells, when corrected for the front side metallization [9]. This high J_{sc} can be related to the excellent FSF, low electrical shading losses and high-quality surface passivation as discussed before.

5 CONCLUSIONS

The results show that high-efficiency IBC cells, with a top efficiency of 19.1%, have been successfully fabricated using low-cost fabrication techniques such as screen printing for patterning to create the p-n regions and metallization. In general the results show higher efficiencies for larger emitter fraction and smaller pitch, with best results in this study obtained for a large emitter fraction of 80% and a small pitch of 2 mm. The cell was passivated with SiO_2+SiN_x:H for the emitter, BSF and gap, and using an excellent FSF and obtaining low electrical shading losses high J_{sc} values of 41.5 mA/cm^2 have been achieved. The IQE values are close to unity in a broad wavelength range. Combining commonly reported *FF* values of around 79% with the obtained values for J_{sc} and V_{oc} in this work would result in cell efficiencies well above 21%. The low *FF* is currently subject of our research effort..

6 REFERENCES

[1] Romijn, I.G., “Back-Contacted Cells for Pilot Line Processing With >19% Efficiency”. Future Photovoltaics, 5, 2011

[2] Castaño, F.J., “Industrially feasible >19% efficiency IBC cells for Pilot Line Processing”. 37th IEEE Photovoltaic Specialist Conference. 2011. Seattle (USA)

[3] Castaño, F.J., “Industrially feasible >19% efficiency IBC cells for Pilot Line Processing”. This conference.

[4] Hermle, M., et al, “Shading Effects in Back-Junction Back-Contacted Silicon Solar Cells”. 33rd IEEE Photovoltaic Specialist Conference. 2008. St. Diego (USA)

[5] Granek, F., “High Efficiency Back-Contact Back-Junction Silicon Solar Cells”. Thesis, 2009

[6] Kim, D.S., et al., “2D-modeling and development of interdigitated back contact solar cells on low-cost substrates”. 4th WCPEC. 2006. Hawaii (USA)

[7] Dicker, J., et al, “Analysis of one-sun monocrystalline rear-contacted silicon solar cells with efficiencies of 22.1%” Journal of Applied Physics, 91, 2002, pp 4335

[8] Dai et al, “A simple general analytical solution for the quantum efficiency of front-surface-field solar cells”. Sol.En.Mat. **43**, 4 ,p363

[9] Guillevin, N., et al, “Development towards 20% efficient Si MWT solar cells for low-cost industrial production”. 1st SiliconPV. 2011. Freiburg (Germany)

[10] Reichel, C., et al., “Investigation of electrical shading effects in back-contacted back-junction silicon solar cells using the two-dimensional charge collection probability and the reciprocity theorem”, J. Appl. Phys. 109, 2011, pp 024507.